ACS APPLIED MATERIALS & INTERFACES

Research Article

www.acsami.org

Long-Lasting Antifog Plasma Modification of Transparent Plastics

Rosa Di Mundo,*[,†,§] Riccardo d'Agostino,[†] and Fabio Palumbo[‡]

[†]Department of Chemistry, University of Bari, via Orabona 4, 70126 Bari, Italy

[‡]Institute for Inorganic Methodologies and Plasmas (IMIP), National Research Council, via Orabona 4, 70126 Bari, Italy

Supporting Information

ABSTRACT: Antifog surfaces are necessary for any application requiring optical efficiency of transparent materials. Surface modification methods aimed toward increasing solid surface energy, even when supposed to be permanent, in fact result in a nondurable effect due to the instability in air of highly hydrophilic surfaces. We propose the strategy of combining a hydrophilic chemistry with a nanotextured topography, to tailor a long-lasting antifog modification on commercial transparent plastics. In particular, we investigated a two-step process consisting of self-masked plasma etching followed by plasma deposition of a silicon-based film. We show that the deposition of the silicon-based coatings on the flat (pristine) substrates allows a continuous variation of wettability from hydrophobic to superhydrophilic, due to a continuous reduction of carbon-containing groups, as assessed by Fourier transform infrared and X-ray photoelectron spectroscopies. By depositing these different coatings on previously nanotextured substrates, the surface wettability behavior is changed consistently, as well as the condensation phenomenon in terms of microdroplets/liquid film appearance. This variation is correlated with advancing and receding water contact angle features of the surfaces. More importantly, in the case of the superhydrophilic coating, though its surface energy decreases with time, when a nanotextured surface underlies it, the wetting behavior is maintained durably superhydrophilic, thus durably antifog.

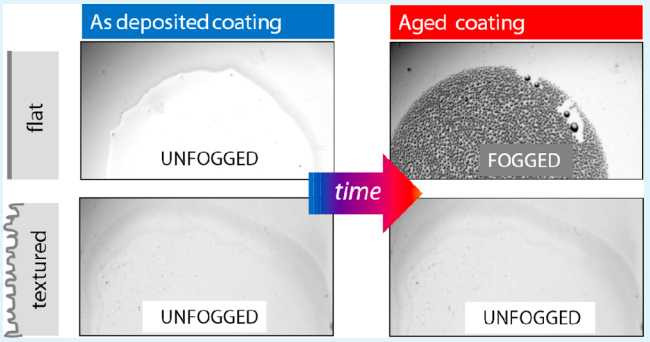

KEYWORDS: *superhydrophilic surface, antifog surface, plasma etching, aging, nanotexturing, transparent plastic, superhydrophobic, silica-like coating*

INTRODUCTION

Antifog surfaces are of high interest since fog formation reduces the effectiveness of light transmission and therefore optical efficiency of transparent materials. This drawback is particularly disabling for optical materials such as eyeglasses, goggles, face shields, and binoculars, not to mention automotive windshields and analytical and medical instruments, or even thermal solar energy converters (windows typically fog due to daily temperature excursion). The reason why water condensation on transparent surfaces turns into a fogging effect has been already thoroughly explained:[1,2] the phenomenon is due to total internal reflection occurring at the water/air interface of condensed droplets when these have a water contact angle higher than a certain threshold value, that is, 48° from Snell's law, thus for any surface with a not marked hydrophilic character. This explains why the approach often used to induce an antifogging behavior on the surface of interest is to increase its surface energy and possibly to make it superhydrophilic. This approach allows the prevention of fogging, whereas defogging solutions are generally based on the increase of air convection.

A common method to induce a nontemporary hydrophilic character for antifog purposes is depositing a thin film from precursors containing hydrophilic functionalities, such as hydroxyl (OH) or carboxyl/ester groups (COOH/COOR). This strategy has been recently utilized by spin coating molecules like poly(ethylene−maleic anhydride) on fused silica substrates[3] or polyacrylate−-colloidal silica on plastic substrates.[4] Also, for application in food packaging, a polysaccharide biopolymer coating (mainly hydroxyl functionalities) has been recently proposed.[5]

Another method is based on the deposition of photochemically active (photosensitive) materials, such as titania (TiO_2), which become superhydrophilic when exposed to radiation.[6]

Layer-by-layer assembling of other hydrophilic inorganic particles such as silica (SiO_2) particles has been tested. Their superhydrophilic properties may be dependent on radiation exposure[7] or sensitive to high temperature.[8] Coatings based on hollow silica−silica nanocomposites, from sol−gel/dip coating methods, have shown antifogging and low reflective properties.[9] Mixed silica/titania nanostructured films from flame deposition or chemical vapor deposition have been also reported.[10,11] High operating temperatures (300−600 °C) are required by most of

Received: July 16, 2014
Accepted: September 8, 2014
Published: September 24, 2014

these methods, so their applicability is limited to quartz/glass materials.[9−11]

Plasma treatments with Ar−O_2 feeds have been also tested directly on optometric lenses to oxidize the carbon chains already present in the substrate.[12]

Though a behavior nearly superhydrophilic (angle <10°) is reached in most of these cases, we highlight that an issue very rarely faced is that of the stability in time of the hydrophilic/superhydrophilic surfaces. When reported, the performance is lost in a short period (20 days,[12] 7 days[13]) and in some cases a renewal of the modification is suggested, for example, with a plasma treatment.[8]

Highly hydrophilic surfaces (water contact angle (WCA) lower than 30°− 40°) are intrinsically unstable in air and tend to reduce the solid/air interfacial energy. This phenomenon is generally named "hydrophobic recovery," since it often refers to polymers (hydrophobic matter) that have been modified to get a hydrophilic surface. It occurs through different "aging" mechanisms driving low-energy groups at the solid surface, often acting simultaneously depending on the surface characteristics: (i) reorientation (through chain rotation or diffusion) of surface functional groups to have the low-energy ones facing the atmosphere and the high-energy ones buried in the bulk of the solid; (ii) absorption on the hydrophilic surface of hydrocarbon molecules present in the atmosphere, as a consequence of their low surface energy.[14]

To prevent the latter effect, stimuli responsive surfaces have been proposed. These, for instance, may present hydrophobic groups beside the hydrophilic ones, which have the role of reducing the adhesion of hydrocarbon molecules.[15] Beside the antifog property, such surfaces have been recently shown to perform the function of separating oil from water in oil−water mixtures.[16]

In this work, we show a different, effective strategy for tailoring on plastic materials (in the present case polycarbonate) a superhydrophilic behavior stable in time. This is based on coupling silicon-based coatings with nanotextured polymer surfaces in a two-step plasma process.

The surface nanotexture, which is randomly rough, is accomplished with a self-nanomasked plasma etching process in a single-step procedure. This has been described elsewhere by these authors for polymers and silicon materials.[17,18] In this process the random roughness generated on the substrate is due to the stochastic deposition on its surface of metal/metal-containing clusters (sputtered from the electrodes or chamber walls upon energetic ion bombardment) which act, along with other eventual nonvolatile species, as a nanomask. Since the masking is caused by the process itself, it is usually called "self"-masking.

In particular, in the case of polymers the nanotexture characteristics have been tuned in combination with a low surface energy chemistry to achieve and investigate superhydrophobicity.[17,19]

In relation to antifog modification of transparent plastics the two-step process hereby described presents also the following advantages: (i) it allows, due to the low operating temperature, unlike many above-cited methods (it is a cold plasma, and the working electrode is not heated), the modification of plastic materials without risk of damage; (ii) due to the smooth control of topography features light scattering can be avoided, preserving transparency of the material (or even to increase it due to reduced reflectance).[19]

In this paper such process is investigated with the aim of effectively evaluating its potential in antifog applications. For this purpose the chemical and, in turn, surface energy tuning of the silicon-based coating is explored as well as the influence of the nanotexture on the final fogging performance and its stability in time.

2. MATERIALS AND METHODS

2.1. Surface Modification. Polycarbonate (PC) substrates (Makrolon 1 mm thick), purchased from GoodFellow, were cut into 1.5 cm × 1.5 cm slices, sonicated in isopropyl alcohol, and dried before processing. Nanotextured PC was prepared in a homemade capacitive coupling (CC) plasma reactor with two parallel stainless steel electrodes with 2 cm gap, the upper one ground and the lower one connected to a radiofrequency (RF, 13.56 MHz, Caesar Dressler) power supply via a matching network. Both electrodes had 140 cm^2 of surface area and were included in a glass vacuum chamber evacuated with a rotative pump (base pressure 0.13 Pa). The gas flow rate was controlled by means of electronic gas flow meters and vacuum measured with a baratron gauge (MKS Instruments). The nanotexturing process, previously optimized,[20] in the present investigation was conducted under the following experimental conditions: PC substrates on the bottom electrode, plasma fed with O_2 at a flow rate of 10 sccm and a working pressure of 13.3 Pa, process duration of 15 min at 100 W. Once etched (nanotextured) with the O_2 plasma, samples were subjected to plasma deposition from a feed containing hexamethyldisiloxane (HMDSO) as monomer. Even if it could be possible to coat the nanotextured samples in the same reactor used for the plasma etching, it was preferred to study the plasma etching and deposition processes in distinct reactors for a more accurate understanding of the role of each step. In particular the deposition step process was carried out in an RF-powered CC plasma reactor with stainless steel chamber, parallel plate electrode configuration (upper electrode 10 cm and lower one 16 cm in diameter, spaced 4 cm apart) where the sample holder is the ground bottom electrode. To gather thin films with wettability in a broad range of WCA, the plasma was fed with an HMDSO/O_2/Ar mixture with monomer and argon flow rate at 1.5 and 50 sccm, respectively, and the following series of experiments were run:

- constant power input, O_2 flow rate varied in the range of 0−100 sccm at the power of 50 W;
- constant O_2 flow rate, RF power changed in the range from 50 to 200 W at an oxygen flow rate of 100 sccm.

Then, the selected coatings were deposited with a thickness of 50 nm (as measured on flat silicon surface) on the textured PC slabs.

2.2. Chemical Characterization. X-ray photoelectron spectroscopy (XPS) analyses of textured PC were carried out by means of Thermo Electron Corporation Theta Probe Spectrometer with a monochromatic Al Kα X-ray source (1486.6 eV) at a spot size of 400 μm. Samples, stored in commercial plastic boxes, were analyzed within 1 d from the processing. Survey (0−1200 eV) and high-resolution spectra (C 1s, O 1s, Si 2p) were acquired at a pass energy of 200 and 150 eV, respectively. Sample charging was corrected with respect to the position of the hydrocarbon component C−C(H), in the C 1s signal. Analyses were typically achieved with a takeoff angle of 53° with respect to surface normal, while when a grazing acquisition was necessary to maximize contribution of the outer layers a 65° takeoff angle was used (25° from the surface).

Fourier Transform infrared (FTIR) absorption spectroscopy analysis of the coatings deposited on polished crystalline silicon was carried out by means of a Bruker Equinox 55 interferometer. Measurements were conducted within 1 h after the deposition, between 500 and 4000 cm^{-1}, with a 4 cm^{-1} resolution. The analysis chamber was purged with a N_2 flux, and the spectra were normalized to film thickness.

2.3. Morphological Characterization. Surface morphology of uncoated and coated samples was investigated by means of scanning electron microscopy (SEM-FEG, Supra 40, Zeiss) with an extraction

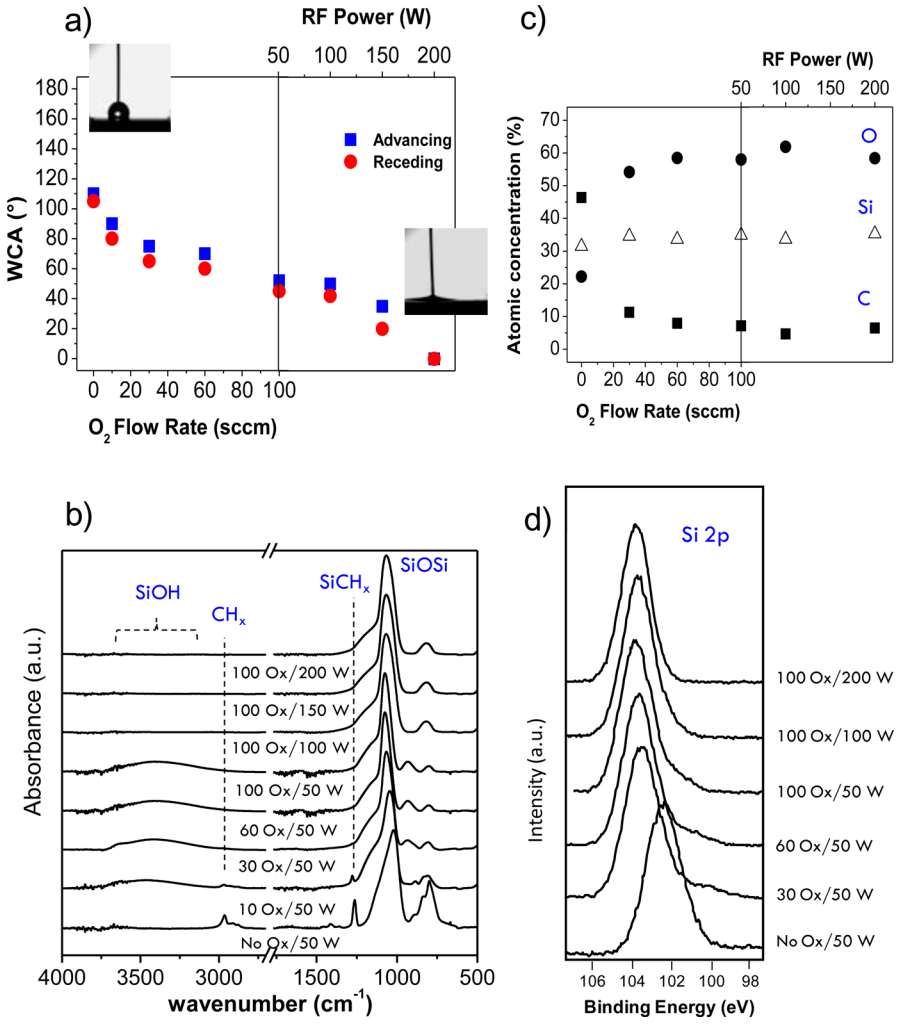

Figure 1. Advancing and receding water contact angle (WCA) of the silicon-based thin films plasma deposited on untreated polycarbonate as a function of plasma conditions (left) oxygen flow rate effect at 50 W and (right) RF power effect at 100 sccm of oxygen flow rate measured within 2 h from the deposition (a); FT-IR spectra (b); XPS atomic percentages (c); Si 2p XPS high-resolution signals of the same films (d).

voltage of 3 kV, both at 0° and 45° tilting angle. Specimens were previously chrome-metalized by sputter coating.

The NTEGRA, NT-MDT Atomic Force Microscope (AFM) was used to obtain quantitative information on surface topography, in particular for the Wenzel roughness factor calculation. Surface (three-dimensional) profiles were acquired in noncontact mode using high accuracy noncontact (HA-NC) "etalon" probes (high aspect ratio tip, cantilever frequency 140 kHz).

2.4. Wetting Measurement. WCA in static and dynamic modes was measured by means of a CAM200 digital goniometer (KSV instruments) equipped with a BASLER A60f camera combined with telecentric zoom optics and LED back lighting. Advancing and receding angles were measured with the sessile drop technique by inducing drop volume variations (from 1 to 4 μL, at a speed of 0.5 μL/s): advancing are the maximum angles observed during the droplet growth; receding angles are the ones just before observation of the contact surface reduction. Each WCA value was averaged from measurements of four drops with an estimated maximum error of 3°. Measurements routinely conducted within 1 h after the modification.

2.5. Condensation Experiment for Fogging Evaluation. Condensation was induced on the modified surfaces by placing the samples on the open top of test tubes containing bidistilled water under heating at 70 °C. Samples were held in that position (with treated surface facing the vapor) for 2 min. At this time they were removed from the vials top and placed in vertical position in the light path, between the lamp and the camera, of the CAM200 digital goniometer (KSV instruments), the same used for WCA measurements, to record in transmission mode the evolution in time of condensed water. Records started in no more than 3 s after that the surface was removed from the vial. The test was conducted at controlled room temperature of 21 °C. An image processing software (ImageJ, NIH) was utilized to make quantitative evaluations on the condensation images. It is worth highlighting that this kind of test for fogging is more restrictive than the relative ASTM protocol (BSEN 166−168), although a direct comparison is not possible due to the different setup: that protocol, in fact, consists in the vapor exposure for 30 s (against 120 s in the method presented in this paper) and defines the material as antifog when it retains 80% of initial transmittance.

3.RESULTS AND DISCUSSION

3.1. Plasma Coatings on Flat Polycarbonate. Figure 1a shows the variation of the advancing and receding WCA, measured within 2 h from the deposition, of the organosilicon thin films plasma deposited on (untreated) polycarbonate slabs as a function of the plasma conditions. Both the effect of oxygen addition and input power were investigated: at constant power, 50 W, oxygen flow rate was increased; then, input power was increased at the maximum oxygen flow rate, 100 sccm. It can be easily appreciated that this approach results in a smooth adjustment of WCA in the range between 0° and 110°. The condition allowing superhydrophilic performance (<5°) is that

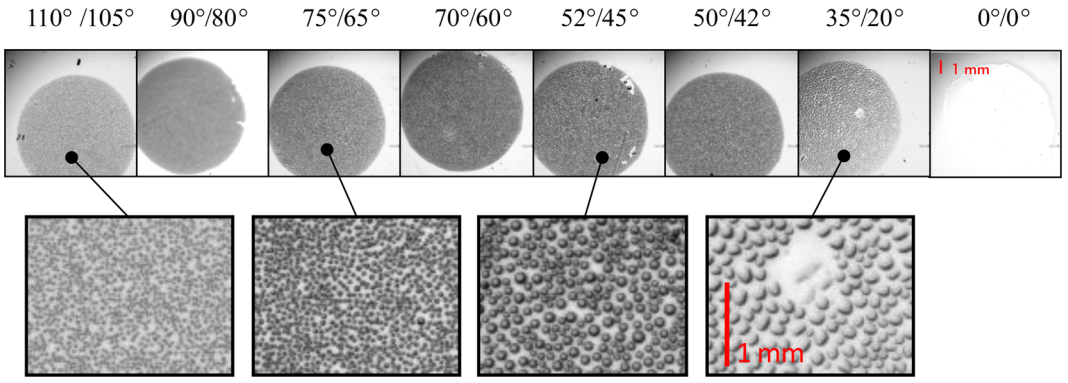

Figure 2. Images of condensed water on flat PC samples coated with the different silicon-based films, just after removal from the vapor-saturated atmosphere. Values of advancing/receding WCA are reported at the top. Higher magnification of some images shows size and distribution of condensed droplets.

obtained at the highest oxygen flow rate and power input; furthermore, it can be observed that in that case WCA is characterized by a very low hysteresis.

Figure 1b reports the FT-IR spectra of the films desposited under the same conditions. The one deposited without oxygen shows the typical IR features of silicone-like coatings, rich in hydrocarbon moieties (indicated by $Si(CH_x)$ and CH_x absorption bands, respectively, at 1260 and 2960 cm^{-1}), while the 200 W prepared film has the well-known inorganic silica-like structure (the only IR features present are related to SiO bonds, at 1070 and 900 cm^{-1}). However, by carefully observing all the spectra of the coatings deposited in the other conditions, the typical behavior of organosilicon plasma deposited films can be appreciated: (i) reduction of hydrocarbon moieties (CH_x, $SiCH_x$) and a significant introduction of SiOH (silanol) groups when oxygen is added at low power, (ii) reduction of silanol groups when power passes from 50 to 100 W, (iii) scarce or no variation when power is further increased, though, as above highlighted, in this range the decrease of WCA (Figure 1a) is still significant.

FTIR outcomes are confirmed by the XPS atomic percentages reported in Figure 1c. The increase of the O-to-Si ratio and the concurrent decrease of the C-to-Si one is that typical of the transition from a silicone- to silica-like composition, occurring when a more effective oxidizing action is exercised by the plasma. The results are in good agreement with the FTIR ones, indicating a steep rise of the O/Si and decrease of the C/Si ratio at low power, when the O_2 flow rate is increased, and limited changes with the power. However, by analyzing the Si 2p high-resolution signals (Figure 1d) it can be appreciated that, though the shift of the peak maximum from 102 to 103.5 eV (in agreement with the oxidation of the coating) is achieved at low oxygen content, the low binding energy component of the signal, ascribed to silicon bonded to carbon and oxygen, is continuously reduced in the entire conditions range considered. Thus, we can conclude that the continuous decrease of WCA observed for these coatings can be due to a progressive increase of SiO_x groups and reduction of $Si(CH)_x$ in the film lattice.

In Figure 2 images resulting from condensation experiments on the flat samples are reported. Pictures were taken as soon as the samples were removed from the top of the vapor-saturated vials and placed in front of the camera. From the low magnification images it can be appreciated that the darkening effect (samples are back-lighted) of condensation sensitively varies as a function of the WCA (values of the advancing/receding angles, plotted in Figure 1a, are reported on the top). The sharpest variation is observed in the case of surfaces with advancing WCA lower than 35° and especially for the 0° surface where a full coalescence to liquid film is observed. For some samples a magnified image is also reported to better appreciate the variation of shape and size of the microdroplets. In particular, as the WCA is reduced, microdroplets reduce in number and increase in size. In particular, the drop diameter increases from around 10 μm, for the most hydrophobic surface, to around 200 μm when the advancing contact angle is equal to 35° (for comparison, the fogging behavior of the untreated PC sample, with WCA of 90°/75°, can be observed in Figure 6, left side).

3.2. Plasma Coatings on Nanotextured Polycarbonate. Figure 3a shows the SEM tilted image of a PC surface

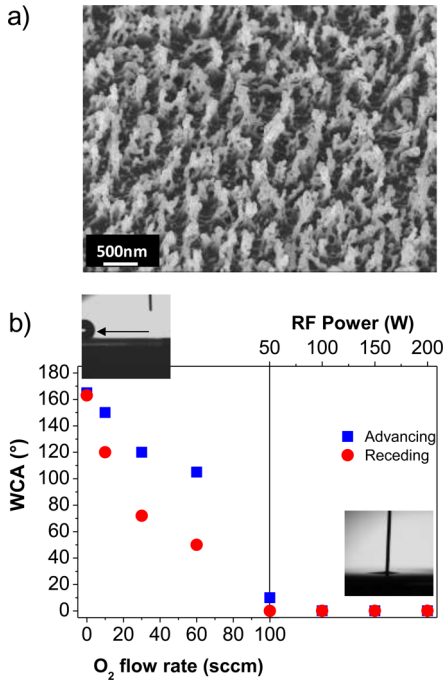

Figure 3. SEM tilted image of PC surface nanotextured with plasma etching and coated with a silica-like coating (a); WCA values measured on nanotextured PC samples coated with different silicon-based films (left) oxygen flow rate effect at 50 W and (right) RF power effect at 100 sccm of oxygen flow rate (b). (insets) Images of the water drop on the two extreme experimental conditions surfaces.

dx.doi.org/10.1021/am504668s | ACS Appl. Mater. Interfaces 2014, 6, 17059−17066

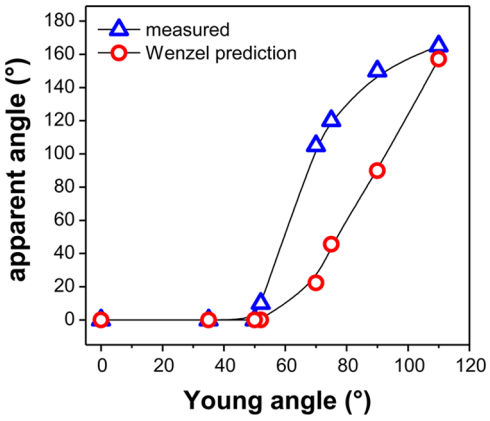

Figure 4. Advancing WCA measured on the nanotextured coated surfaces (apparent angle) as a function of the advancing WCA of the corresponding coated flat surfaces (Young angle). The apparent angle as calculated according to the Wenzel equation (with r_W calculated from AFM data Supporting Information, Figure SI2) is reported for a comparison with theory.

nanotextured with an O_2-fed plasma etching and coated with a silica-like coating. The plasma etching was conducted according a procedure elsewhere described,[20] under the selected condition of 15 min and 100 W, which results in relatively deep texturing (about 640 nm high and 150 nm wide structures) though preserving sample transparency. No difference could be appreciated in SEM images of nanotextured and coated PC surfaces under the examined deposition conditions.

In Figure 3b the WCA values measured on textured PC samples, coated with the silicon-based films described in the previous section, are reported. It can be easily perceived that on the textured surface the range of WCA is enlarged: wetting goes from low-hysteresis superhydrophobic (also indicated as superhydrorepellent, slippery superhydrophobic) to superhydrophilic. In particular, it can be observed that WCA steeply decreases (showing significant hysteresis values) at 50 W as the amount of added oxygen is increased: a superhydrophilic character is reached at such a low power value at the highest oxygen flow rate. The achieved superhydrophilic wetting behavior appears as a regime elsewhere described as "permeation" (or liquid–solid Cassie) regime,[21] that is, a regime where grooves are completely filled by water also beyond the drop profile, as indicated by the particular water spreading observed during WCA measurement (video of the 100 O_2, 200 W sample in the Supporting Information SI1).

In Figure 4 the advancing WCA of the textured coated surfaces (apparent angle, θ_{app}) is plotted as a function of the advancing WCA of the corresponding flat coated surfaces (Young angle, θ_Y). In the same diagram the apparent angle calculated according to the Wenzel equation[22] ($\cos \theta_{app} = r_W \cos \theta_Y$, with r_W calculated from AFM data, Supporting Information, Figure SI2) is reported for each condition. This way, it is possible to better appreciate that, in agreement with the equation for $\theta_Y \leq 50°$, θ_{app} is invariantly equal to 0°. However, for $50° < \theta_Y < 90°$, contrary to Wenzel prediction, apparent angles of textured surfaces are raised and not lowered with respect to the corresponding θ_Y. This seems to indicate that, in this θ_Y range, water establishes a composite Cassie–Baxter-like contact with the textured surface, since the combination of surface energy and protrusion size inhibits liquid permeation, and air is trapped underneath. This could explain also the deviation at $\theta_Y = 90°$, for which the found apparent angle is much higher than the corresponding Wenzel value.

Condensation measurement pictures of the coated textured samples with WCA values of Figure 3b are reported in Figure 5. Also in this case a transition to liquid film (thus "invisible") condensation is observed as the surface turns to superhydrophilic, which as above-described, for a textured surface occurs for coatings deposited at RF power higher than 50 W. Interestingly, contrary to condensation on flat samples (Figure 2) for the textured ones a darkening is observed when the advancing WCA passes from 165° to 105°. This may be reasonably a consequence of the broadening in this range of the WCA hysteresis, higher than the one observed on flat samples. High values of WCA hysteresis, as is well-known, indicate the existence of a strong adhesion force between the liquid and the solid surface,[23] which hinders water motion. This way not only drop coalescence is hindered but also an irregular shape is induced on the microdroplets (evident in the magnified image of the surface with 105°/50° advancing/receding angle), which results in a more pronounced scattering of the light. This had been already suggested by scholars investigating corona-treated polyethylene characterized by different WCA and WCA hysteresis values.[2] Thus, not only contact angle, but also its hysteresis affects light transmission of fogged transparent materials.

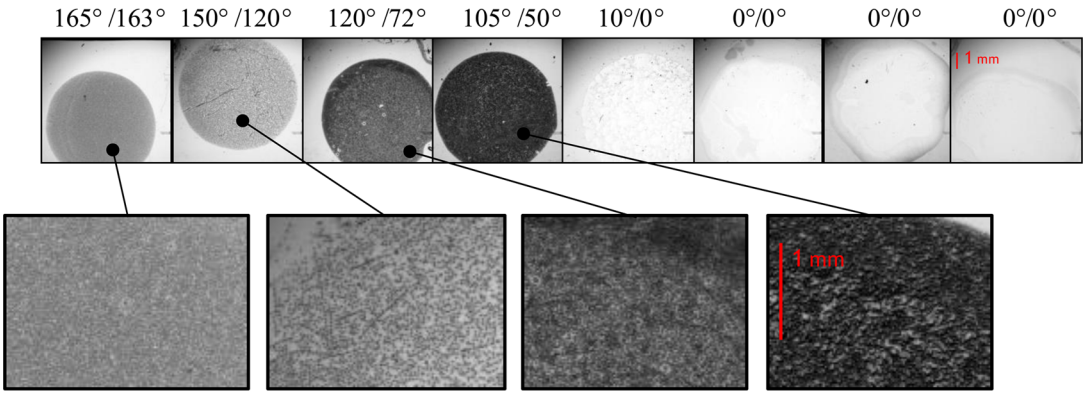

Figure 5. Images of condensed water on PC samples nanotextured with plasma etching and coated with the different silicon-based films. Higher magnification images of the dropwise condensing (fogged) surfaces are shown below. Values of advancing/receding WCA are reported at the top.

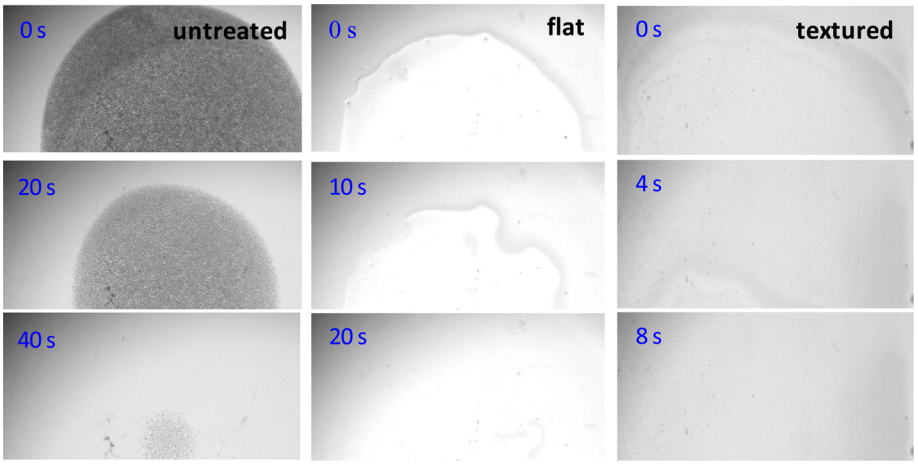

Figure 6. Time-lapse sequence of condensed water on the superhydrophilic film (100 sccm oxygen, 200 W) coated flat PC (in the middle) and on the superhydrophilic nanotextured PC (same film, on the right). For comparison, the sequence for the untreated sample is reported on the left. The different appearance of the film-wise condensation can be noticed on flat and textured superhydrophilic surfaces.

It is worth noticing that the here-shown influence of the Young angle (in its whole range) on the condensation phenomenon of flat and textured surfaces (Figures 2 and 5), though investigated in this work for antifog purposes, could be useful also for applications requiring dropwise condensation rather than a liquid-wise one.[24,25] It is also interesting to note that the dropwise condensation observed on superhydrophobic surfaces has been recently reported by other authors to show an antifog functionality at low temperature, beside the anti-icing one, since condensed droplets can be easily removed from the surface by tilting or slightly blowing.[26]

Another aspect relevant to antifogging of transparent surfaces is the time necessary for dewetting, that is, the time necessary to achieve a full evaporation of condensed water, thus completely restoring the initial condition. Figure 6 reports the time-lapse sequence of condensed water on the most hydrophilic (100 sccm of oxygen-200W) flat sample compared to the most hydrophilic textured one (same coating). For comparison, the sequence for the untreated sample is reported. Both samples, as already highlighted, do not show darkening (fogging) effects upon condensation, thus display an antifog performance. However, for the textured sample a faster drying is observed (8 s vs 20 s). This is likely a consequence of the increased surface area due to nanotexture, which leads to a thinner liquid film and quickens the evaporation.

Another relevant observation can be drawn: water condensed on the nanotextured sample, responsible for the permeation regime, does not introduce light transmittance difference between wet and unwet portion of the surface, whereas for the flat sample a neat brightening in the wet region can be perceived. All these features allow to consider the superhydrophilic textured samples better behaving as antifog materials.

3.3. Aging Effect Comparison. Figure 7a reports the advancing/receding WCA values measured on the flat-coated PC surfaces after four months from the deposition (preparation); the gray markers on the diagram are those relative to the measurements performed soon after the plasma modification. Notice that a marked aging occurs in surfaces with a WCA angle lower than 50°, in particular, in those with a superhydrophilic character. This kind of "hydrophobic transition" relates to the well-known instability of high-energy surfaces, which has been thoroughly reported for surface-

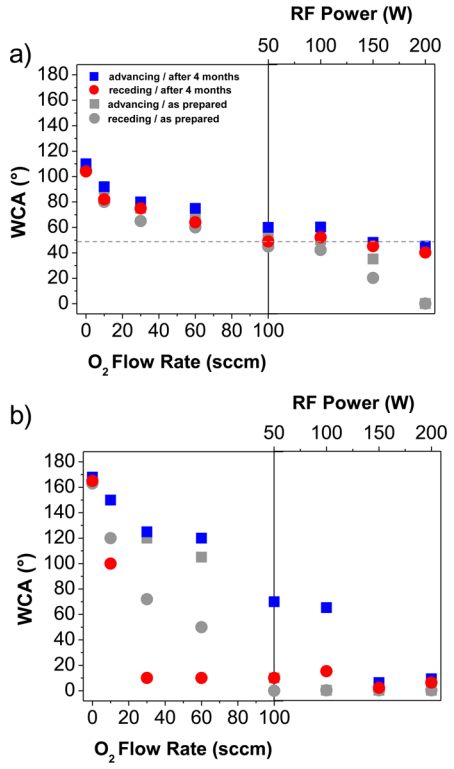

Figure 7. Advancing/receding WCA values measured on flat-coated PC surfaces after four months from the deposition (a) and on textured-coated surfaces after the same period (b) (left) oxygen flow rate effect at 50 W (right) RF power effect at 100 sccm of oxygen flow rate. Gray markers on the diagrams refer to the measurements performed soon after the plasma modification (Figure 1a and 3b).

modified polymers, but rarely on silica-like surfaces (thus often found as hydrophobic recovery). To explain this behavior a grazing-angle XPS analysis was performed on the most hydrophilic sample (100 sccm O_2, 200W) at the aging time considered, and description is reported in the Supporting Information, Figure SI4. The XPS results point to the evolution with time of hydrocarbon adsorption as being responsible for the WCA variation. Thus, the aging behavior of the superhydrophilic silica coating makes it not suitable per se for

dx.doi.org/10.1021/am504668s | ACS Appl. Mater. Interfaces 2014, 6, 17059−17066

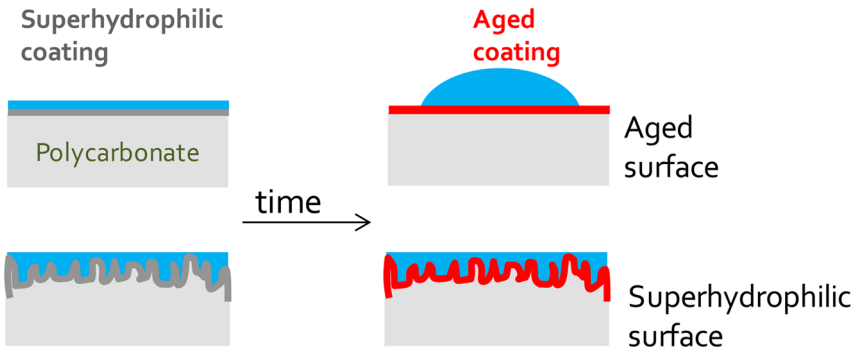

Figure 8. Simplified scheme showing how surface texture ensures a durable superhydrophilic performance by hiding the chemical variations (surface energy decrease) suffered by the coating.

an antifog long-lasting modification. In Figure 7b the WCA values measured after the same period on the textured coated surfaces are reported. Notice, with respect to the as treated samples (Figure 3b), a huge increase in WCA hysteresis for all samples except for the extreme ones; for the hydrophilic samples this is a consequence of the increase of the advancing angle upon aging, while the receding remains low (typical effect of hydrophilic surfaces).[27]

It is important to remark that the superhydrophilic samples do not show such a variation, so they are stable in wetting performance at the time considered (four months in the diagram, but for these samples, stability even at one year has been assessed). This durability is much longer than that, when reported, shown by superhydrophilic surfaces fabricated by other methods.[7,10,11] This behavior can be explained by carefully considering the relationship between apparent and young angle in textured surfaces reported in Figure 4: even if the young angle at the aging time considered (WCA of Figure 7a) reaches the value of 50° (and this actually happens) the apparent angle keeps staying at low values. Therefore, as sketched in Figure 8, texture turns off the aging effect since it hides the chemical variations suffered by the coating.

4. CONCLUSION

In this work we have investigated a two-step process, consisting of a combination of a self-masked plasma etching and a silica-like film plasma deposition, to tailor a permanent antifog modification on a commercial transparent polycarbonate. The first step has the role of texturing at the nanoscale the plastic substrate, while the second one imparts the necessary high surface energy to the material.

We have found that the deposition of the silica-like coating is smoothly tunable by varying plasma parameters to get a continuous variation of WCA in the range of 0−110°: coatings with WCA of 0° induce film-wise water condensation, thus resulting in an antifog behavior. However, this performance is not stable in time due to the decrease of surface energy (hydrophobic transition); this fact, unless renewing procedures are used, make the mere silica deposition not suitable as a permanent antifog treatment. When the plastic substrate is nanotextured before the silica deposition a long-lasting (tested up to one year) superhydrophilic, and in turn antifog, modification can be obtained, as a consequence of the influence of roughness on the apparent angle, even when the young angle has increased by aging.

This durability of superhydrophilicity is particularly rare in related literature. This allows the proposal of this combined plasma procedure, which is also simple and implementable on the same reactor, as an advantageous method for antifog modification of transparent plastics.

■ ASSOCIATED CONTENT

Ⓢ Supporting Information

Water contact angle of superhydrophilic textured surface and permeation effect, AFM image of nanotextured surface and Wenzel roughness factor (r_w) calculation, transparency and drying velocity, grazing-angle XPS of the superhydrophilic coating as deposited and after four months of storage in air, and .avi files. This material is available free of charge via the Internet at http://pubs.acs.org/.

■ AUTHOR INFORMATION

Corresponding Author

*E-mail: rosa.dimundo@poliba.it.

Present Address

[§]Dipartimento di Meccanica, Matematica e Management, Politecnico di Bari, v.le Japigia 182, 70126 Bari, Italy.

Author Contributions

The manuscript was written through contributions of all authors. All authors have given approval to the final version of the manuscript.

Funding

This work was financially supported by the Apulia Region fundings "Laboratorio Pubblico di Ricerca Industriale Pugliese dei Plasmi-LIPP."

Notes

The authors declare no competing financial interest.

■ ACKNOWLEDGMENTS

G. Carbone (Dipartimento di Meccanica, Matematica e Management, Politecnico di Bari) is gratefully acknowledged for the assistance in topography data calculations. D. Cappelluti and M. Troia are acknowledged for their support in texturing and condensation experiments.

■ REFERENCES

(1) Briscoe, B. J.; Galvin, K. P. The Effect of Surface Fog on the Transmittance of Light. *Sol. Energy* **1991**, *46*, 191−197.

(2) Briscoe, B. J.; Williams, D. R.; Galvin, K. P. Condensation on Hydrosol Modified Polyethylene. *Colloids Surf., A* **2005**, *264*, 101−105.

(3) Chevallier, P.; Turgeon, S.; Sarra-Bournet, C.; Turcotte, R.; Laroche, G. Characterization of Multilayer Anti-Fog Coatings. *ACS Appl. Mater. Interfaces* **2011**, *3*, 750−758.

(4) Chang, C.-C.; Huang, F.-H.; Chang, H.-H.; Don, T.-M.; Chen, C.-C.; Cheng, L.-P. Preparation of Water-Resistant Antifog Hard Coatings on Plastic Substrate. *Langmuir* **2012**, *28*, 17193−17201.
(5) Introzzi, L.; Fuentes-Alventosa, J.-M.; Cozzolino, C. A.; Trabattoni, S.; Tavazzi, S.; Bianchi, C. L.; Schiraldi, A.; Piergiovanni, L.; Farris, S. Wetting Enhancer" Pullulan Coating for Antifog Packaging Applications. *ACS Appl. Mater. Interfaces* **2012**, *4* (7), 3692−3700.
(6) Zhang, J.; Severtson, S. J. Fabrication and Use of Artificial Superhydrophilic Surfaces. *J. Adhes. Sci. Technol.* **2014**, *28*, 751−768.
(7) Han, J. T.; Kim, S.; Karim, A. UVO-Tunable Superhydrophobic to Superhydrophilic Wetting Transition on Biomimetic Nanostructured Surfaces. *Langmuir* **2007**, *23*, 2608−2614.
(8) Cebeci, F. C.; Zhizhong, W.; Zhai, L.; Cohen, R. E.; Rubner, M. F. Nanoporosity-Driven Superhydrophilicity: A Means to Create Multifunctional Antifogging Coatings. *Langmuir* **2006**, *22*, 2856−2862.
(9) Zhang, X.; Lan, P.; Lu, Y.; Li, J.; Xu, H.; Zhang, J.; Lee, Y. P.; Rhee, J. Y.; Choy, K. L.; Song, W. Multifunctional Antireflection Coatings Based on Novel Hollow Silica−Silica Nanocomposites. *ACS Appl. Mater. Interfaces* **2014**, *6* (3), 1415−1423.
(10) Tricoli, A.; Righettoni, M.; Pratsinis, S. E. Anti-Fogging Nanofibrous SiO_2 and Nanostructured SiO_2-TiO_2 Films Made by Rapid Flame Deposition and In Situ Annealing. *Langmuir* **2009**, *25*, 12578−12584.
(11) Chen, Y.; Zhang, Y.; Shi, L.; Li, J.; Xin, Y.; Yang, T.; Guo, Z. Transparent Superhydrophobic/Superhydrophilic Coatings for Self-Cleaning and Anti-Fogging. *Appl. Phys. Lett.* **2012**, *101*, 033701−033704.
(12) Grosu, G.; Andrzejewski, L.; Veilleux, G.; Ross, G. G. Relation Between the Size of Fog Droplets and Their Contact Angles with CR39 Surfaces. *J. Phys. D: Appl. Phys.* **2004**, *37*, 3350−3355.
(13) Patel, P.; Choi, C. K.; Desheng, M. D. Superhydrophilic Surfaces for Antifogging and Antifouling Microfluidic Devices. *JALA (1998-2010)* **2010**, *15*, 114−119.
(14) Garbassi, F.; Morra, M.; Occheillo, E. *Polymer Surfaces from Physics to Technology;* Wiley: Chichester, U.K., 1994.
(15) Howarter, J. A.; Youngblood, J. P. Self-Cleaning and Next Generation Anti-Fog Surfaces and Coatings. *Macromol. Rapid Commun.* **2008**, *29*, 455−466.
(16) Brown, P. S.; Atkinson, O. D. L. A.; Badyal, J. P. S. Ultrafast Oleophobic−Hydrophilic Switching Surfaces for Antifogging, Self-Cleaning, and Oil−Water Separation. *ACS Appl. Mater. Interfaces* **2014**, *6* (10), 7504−7511.
(17) Di Mundo, R.; Palumbo, F.; d'Agostino, R. Influence of Chemistry on Wetting Dynamics of Nanotextured Hydrophobic Surfaces. *Langmuir* **2010**, *26*, 5196−5201.
(18) Di Mundo, R.; Palumbo, F.; Barucca, G.; Sabato, G.; d'Agostino, R. On the "Growth" of Nano-Structures on c-Silicon Via Self-Masked Plasma Etching Processes. *Plasma Processes Polym.* **2013**, *10*, 843−849.
(19) Di Mundo, R.; Troia, M.; Palumbo, F.; Trotta, M.; d'Agostino, R. Nano-texturing of Transparent Polymers with Plasma Etching: Tailoring Topography for a Low Reflectivity. Plasma. *Plasma Processes Polym.* **2012**, *9*, 947−954.
(20) Palumbo, F.; Di Mundo, R.; Cappelluti, D.; d'Agostino, R. SuperHydrophobic and SuperHydrophilic Polycarbonate by Tailoring Chemistry and Nano-texture with Plasma Processing. *Plasma Processes Polym.* **2011**, *8*, 118−126.
(21) Quéré, D. Non-sticking drops. *Rep. Prog. Phys.* **2005**, *68*, 2495−2532.
(22) Wenzel, R. N. Surface Roughness and Contact Angle. *J. Phys. Chem.* **1949**, *53*, 1466−1470.
(23) Furmidge, C. L. G. Studies at Phase Interfaces. I. The Sliding of Liquid Drops on Solid Surfaces and a Theory for Spray Retention. *J. Colloid Sci.* **1962**, *17*, 309.
(24) Macner, A. M.; Daniel, S.; Steen, P. H. Condensation on Surface Energy Gradient Shifts Drop Size Distribution toward Small Drops. *Langmuir* **2014**, *30*, 1788−1798.
(25) Paxson, A. T.; Yagüe Jose, L.; Gleason, K. K.; Varanasi, K. K. Stable Dropwise Condensation for Enhancing Heat Transfer via the Initiated Chemical Vapor Deposition (iCVD) of Grafted Polymer Films. *Adv. Mater.* **2014**, *26*, 418−423.
(26) Wen, M.; Wang, L.; Zhang, M.; Jiang, L.; Zheng, Y. Antifogging and Icing-Delay Properties of Composite Micro- and Nanostructured Surfaces. *ACS Appl. Mater. Interfaces* **2014**, *6* (6), 3963−3968.
(27) Di Mundo, R.; Palumbo, F. Comments Regarding 'An Essay on Contact Angle Measurements'. *Plasma Processes Polym.* **2011**, *8*, 14−18.